# SMALL STRAIN SHEAR STIFFNESS OF TOYOURA SAND OBTAINED FROM VARIOUS WAVE MEASUREMENT TECHNIQUES

Ruta Ireng WICAKSONO[1] and Reiko KUWANO[2]

**ABSTRACT**: This paper compiles the values of shear modulus on Toyoura sand evaluated in laboratory tests by 6 researchers using various techniques in Institute of Industrial Science, the University of Tokyo in the last 5 years. In total, six measurement techniques including static, Trigger Accelerometer (TA) with S wave, TA with P wave, Bender Element, S type Plate Transducer (PT) method and P type PT method were performed in this study. As the results, for each measurement method the values of normalized shear modulus (G/f(e)) were in a good agreement having the deviation at largest of about 7.6%. Further study on the TA methods employing accelerometers inside and outside the specimens was reported. Additionally, the shear modulus values resulted from this study and those from International Parallel Test on the Measurement of $G_{max}$ using Bender Elements organized by TC-29 were compared.

**Keywords**: small strain, cyclic loading, trigger accelerometer, bender element, plate transducer

## INTRODUCTION

In the field at construction sites, wave measurement techniques such as the cross-hole and down-hole methods, have been used for a long time to obtain small strain stiffness of the ground (Stokoe & Hoar, 1978). Meanwhile, in mega project of Akashi Kaikyo Bridge, Tatsuoka & Kohata (1995) presented stiffness modulus by employing pressure meter and plate loading tests as an in-situ static measurement that yields the shear modulus in larger strain.

For long time a laboratory measurement has become the reference standard for determining the properties of geomaterials. To develop a greater confidence of the results from an in-situ test, it is helpful to compare the field results with the laboratory ones. In case of a laboratory static measurement, established method of vertically and torsionally cyclic loading performed by triaxial and torsional apparatuses respectively has been employed in obtaining the stiffness modulus values. Additionally, in most of the studies (Dyvik and Madshus (1985), Mohsin and Airey (2003), and Lee and Santamarina (2005)), a bender element was employed to measure the shear wave velocity in a laboratory.

From those kinds of measurement, a disputable issue emerges in decades to the definitions of "static properties" and "dynamic properties". Woods (1991) proposed not to use "dynamic properties", since dynamic concerns the loading condition. He also suggested that there is no more different from

―――――――――――――――――――――

[1] Graduate student, The University of Tokyo, Japan, ruta@iis.u-tokyo.ac.jp

[2] Associate Professor, The University of Tokyo, Japan, kuwano@iis.u-tokyo.ac.jp

each other except for the strain levels. However, precise static small strain measurements in the laboratory tests have bridged the gap of strain levels between "dynamic" and "static" behavior (Tatsuoka and Shibuya, 1992). Following the pioneer work by Tanaka et al. (2000), AnhDan and Koseki (2002) found that the difference on dynamic and static properties is not only caused by strain level but also by some other factors like grain size and wave length. Nevertheless, in accordance with the definition by Tatsuoka and Shibuya (1991), in this paper the terms of static and dynamic measurements are used with respect to the effects of inertia to the soil particles during the testing.

Geotechnical Engineering Laboratory in Institute of Industrial Science (IIS), The University of Tokyo has been taking part together with other labs around the world exploring the soil and geotechnical-related behaviors both in field and laboratory. Particularly in laboratory work, small strain stiffness measurement has been becoming one of hot topics in this lab, while several researchers have been performing this work with various techniques on Toyoura sand.

With respect to that, this study aims to compile and comprehensively to compare the values of shear modulus of Toyoura sand from those works in the last 5 years. Triaxial Compression (TC) and Torsional Shear (TS) tests were performed to observe small strain cyclic loading which is known as a static measurement. Meanwhile for a dynamic measurement, independent tools of Trigger Accelerometer (TA), Bender Element (BE), and Plate Transducer (PT) were employed, that were attached to triaxial and torsional apparatuses as additional tools.

## MATERIAL, APPARATUS, AND TESTING PROCEDURES

### Material
Material used in this study was Toyoura sand from batch H owned by the Geotechnical Engineering Laboratory in IIS. This sand was taken from Toyoura Beach, Yamaguchi, Japan. Toyoura sand is fine uniform sand that has been widely used in geotechnical engineering laboratories all over Japan. Its mean diameter ($D_{50}$) is 0.2 mm. The specific gravity Gs is 2.635. The maximum void ratio $e_{max}$ is 0.966 and the minimum void ratio $e_{min}$ is 0.600.

### Apparatus
In this study, both fully automated triaxial and torsional apparatuses were employed. Small, medium, and large scales of apparatus size were used appropriately adapting to the specimen size. Figure 1 shows the schematic figure of the triaxial apparatus used in this study, while that only in loading system and specimen shape the torsional apparatus differs.

As shown in Figure 1, the basic components of the system consist of a triaxial cell with a pneumatic cell pressure system, loading system, transducers and a personal computer equipped with a control and measurement program. A personal computer is connected to the apparatus through cards having 2 major functions of data acquisition and feed back control units. External Displacement Transducer (EDT) is utilized to measure the overall height of the specimen. A High Capacity Differential Pressure Transducer (HCDPT) is used to measure effective confining pressure in the cell. A Low Capacity Differential Pressure Transducer (LCDPT) which is connected with 2 water-filled burettes is employed to measure the volumetric strain of the specimen. One burette is connected to the specimen, while the other performs as a reference. The volume change is evaluated by measuring the difference in the water-head between those burettes.

A set of tools such as TA, BE, or PT was used for a dynamic measurement which is independently attached to the triaxial or the torsional apparatus. Figures 2a and 2b show the photos of TA and BE attached to the triaxial apparatus. Meanwhile, the units of PT where their positions on top cap and pedestal respectively are replaceable with those of BE, is shown in Figure 2c.

Those dynamic measurement tools are connected to several supporting devices including function generator, signal amplifier, charge amplifier, and digital oscilloscope. The function generator is employed to produce the P and the S waves signal. Both excitation types of pulse and sinusoidal waves can be generated and are sent to a trigger or a transmitter through a signal amplifier. To magnify the signal captured by the sensor, a charge amplifier is used and then its output is connected to a digital

oscilloscope for recording.

Additionally, a pair of widely used Local Deformation Transducer (LDT) after Goto et al. (1991) was employed to perform small strain cyclic loading. As shown in Figure 2b, the LDT is attached to the specimen through 2 pairs of hinge that are fixed with glue on the membrane. The length of the LDT varies with the size of the specimen.
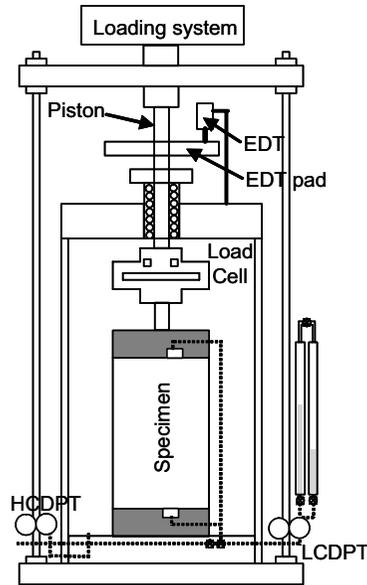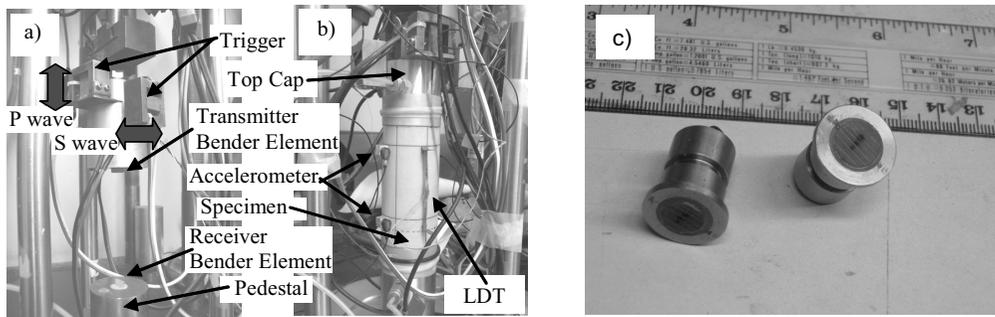


Figure 1. Schematic figure of TC apparatus



Figure 2. a) Trigger and Bender Element positions; b) Accelerometer & LDT position; c) Plate transducer

### *Testing Procedures*

Air dried Toyoura sand was pluviated through air from a certain height to obtain the designed dry density. Cylindrical specimen at several sizes for TC test and hollow specimen for TS test were prepared under both dry and saturated conditions. After completing the preparation stage, the specimen was subjected stepwise to several stress levels under specific condition of isotropic consolidation in some cases, while that of anisotropic one in other cases.

At each stress level, the work of probing small strain stiffness by the ways of static and dynamic measurements was carried out. Among the static and dynamic measurements, a stage with constant

stress state in a couple minutes for stabilization was conducted. For static measurement, a cyclic loading stage was conducted under drained condition by changing the vertical stress in TC test case, while that by changing the shear stress in TS test case. For dynamic measurement, the elastic wave that propagates through the specimen was produced and was captured respectively by the trigger/transmitter and the sensors. A digital oscilloscope was employed in recording the wave time history.

Table 1 summarizes some important information of researchers, apparatuses, specimen size, the condition of specimen, specimen density, and the observed gain.

Table 1 Data of specimens

| # | Researcher | Apparatus | Specimen size* | Condition | Dr** | Observed gain |
|---|---|---|---|---|---|---|
| A1 | Wicaksono, R.I. | Triaxial | $\varnothing = 100$ ; h = 200 | Dry | 88.5 | $E_{TC}$, $E_{TA-P}$ |
| A2 | Wicaksono, R.I. | Triaxial | $\varnothing = 50$ ; h = 100 | Saturated | 67.8 | $E_{TC}$, $G_{BE}$, $G_{TA-S}$, $E_{TA-P}$ |
| A3 | Wicaksono, R.I. | Triaxial | $\varnothing = 50$ ; h = 100 | Dry | 86.9 | $E_{TC}$, $G_{BE}$, $G_{TA-S}$, $E_{TA-P}$ |
| A4 | Wicaksono, R.I. | Triaxial | $\varnothing = 300$ ; h = 600, $t_{membrane} = 0.8$ | Dry | 74.5 | $E_{TC}$, $G_{TA-S}$, $E_{TA-P}$ |
| B1 | De Silva, L.I.N. | Torsional | $\varnothing_{outer} = 150$, $\varnothing_{inner} = 90$ ; h = 300 | Saturated | 77.9 | $G_{TS}$ |
| B2 | De Silva, L.I.N. | Torsional | $\varnothing_{outer} = 150$, $\varnothing_{inner} = 90$ ; h = 300 | Saturated | 56.8 | $G_{TS}$ |
| B3 | De Silva, L.I.N. | Torsional | $\varnothing_{outer} = 150$, $\varnothing_{inner} = 90$ ; h = 300 | Dry | 74.9 | $E_{TS}$ |
| B4 | De Silva, L.I.N. | Torsional | $\varnothing_{outer} = 150$, $\varnothing_{inner} = 90$ ; h = 300 | Dry | 38.3 | $E_{TS}$ |
| B5 | De Silva, L.I.N. | Torsional | $\varnothing_{outer} = 150$, $\varnothing_{inner} = 90$ ; h = 300 | Dry | 68.6 | $G_{TA-S}$ |
| C1 | Mulmi, S. | Triaxial | $\varnothing = 50$ ; h = 180 | Dry | 91.0 | $E_{TA-P}$, $G_{BE}$, $G_{TA-S}$ |
| C2 | Mulmi, S. | Triaxial | $\varnothing = 30$ ; h = 100 | Dry | 83.6 | $E_{TC}$, $G_{BE}$ |
| C3 | Mulmi, S. | Triaxial | $\varnothing = 40$ ; h = 100 | Dry | 82.0 | $E_{TC}$, $G_{BE}$ |
| C4 | Mulmi, S. | Triaxial | $\varnothing = 50$ ; h = 100 | Dry | 88.3 | $G_{PT-S}$ |
| C5 | Mulmi, S. | Triaxial | $\varnothing = 50$ ; h = 100 | Dry | 86.6 | $E_{PT-P}$ |
| D1 | Enomoto, T. | Triaxial | $\varnothing = 300$ ; h = 600, $t_{membrane} = 0.8$ | Dry | 98.4 | $E_{TC}$, $G_{TA-S}$ |
| D2 | Enomoto, T. | Triaxial | $\varnothing = 300$ ; h = 600, $t_{membrane} = 2.0$ | Dry | 98.8 | $E_{TC}$, $G_{TA-S}$ |
| E1 | Kiyota, T. | Triaxial | $\varnothing = 50$ ; h = 100 | Saturated | 85.0 | $E_{TC}$, $G_{TA-S}$ |
| E2 | Kiyota, T. | Torsional | $\varnothing_{outer} = 150$, $\varnothing_{inner} = 90$ ; h = 300 | Saturated | 70.5 | $G_{TA-S}$ |
| F1 | Tsutsumi, Y. | Triaxial | $\varnothing = 50$ ; h = 100 | Dry | 42.1 | $E_{TC}$, $G_{BE}$, $G_{TA-S}$, $E_{TA-P}$ |
| F2 | Tsutsumi, Y. | Triaxial | $\varnothing = 50$ ; h = 100 | Dry | 73.5 | $E_{TC}$, $G_{BE}$, $G_{TA-S}$, $E_{TA-P}$ |
| F3 | Tsutsumi, Y. | Triaxial | $\varnothing = 50$ ; h = 100 | Dry | 77.9 | $E_{TC}$, $G_{BE}$, $G_{TA-S}$, $E_{TA-P}$ |
| R47 | Wicaksono, R.I. | Triaxial | $\varnothing = 300$ ; h = 600, $t_{membrane} = 0.8$ | Dry | 98 | $E_{TC}$, $G_{TA-S}$, $E_{TA-P}$ |

* Specimen size in mm;    ** Relative density (Dr) in %

*Source*: Data A1- A3 (Wicaksono, 2007a); Data B (De Silva et al., 2005); Data C1 - C3 (Mulmi et al., 2008a) ; Data C4 - C5 (Mulmi et al., 2008b), Data D (Enomoto, 2008), Data E (Kiyota, 2008), Data F (Tsutsumi et al., 2006)

## DATA PREPARATION

In this study, values of Young's modulus (E) and shear modulus (G) were observed from static and dynamic measurements. The values of E were observed from the cyclic loading of TC test, and as well, from evaluating of P wave velocity obtained from TA method with P wave and P type PT method that result in the values of $E_{TC}$, $E_{TA-P}$, and $E_{PT-P}$, respectively. Note that the value of $E_{PT-P}$ was observed indirectly as explained next in this section. Meanwhile, the values of G were observed from the TS test, the TA with S wave, the BE, and the S type PT methods that result in the values of $G_{TS}$, $G_{TA-S}$, $G_{BE}$, and $G_{PT-S}$, respectively.

In static measurement, the values of E and G are observed by employing Equations 1 and 2 for the data obtained from TC and TS tests, respectively, as follows:

$$E = \frac{\Delta \sigma_V}{\Delta \varepsilon_V} \tag{1}$$

$$G = \frac{\Delta \tau}{\Delta \gamma} \tag{2}$$

where $\Delta \varepsilon_v$ is the increment of vertical strain corresponding to the increment of vertical stress ($\Delta \sigma_v$) during the cyclic loading in TC test. Meanwhile, $\Delta \gamma$ is the increment of shear strain corresponding to

the increment of shear stress ($\Delta\tau$) during the cyclic loading in TS test.

In dynamic measurement with the TA method using P wave, by presuming that the triggers are fixed to the top cap rigidly, an unconstrained wave in longitudinal direction that propagates in the rod is assumed. Hence, the value of E is observed by employing Equation 3 after evaluating P wave velocity ($V_P$) and by knowing density of the specimen ($\rho$), as follows:

$$E = \rho \cdot V_P^2 \qquad (3)$$

With the TA method using S wave, under similar presumption about the behavior of the triggers and the top cap as previously, the elastic wave that propagates in torsional direction on the transverse section of the rod is assumed. Since the stiffness that controls shear wave in the rod is the same as in an infinite continuum, the velocity of torsional wave is the same as for body S wave (Santamarina, 2001). Meanwhile in the BE and the S type PT methods, S wave that propagates from the source to the receiver is considered as point to point propagation in an infinite continuum. Therefore, after evaluating S wave velocity ($V_S$) and by knowing density of the specimen ($\rho$), the value of G is observed by employing Equation 4, as follows:

$$G = \rho \cdot V_S^2 \qquad (4)$$

Meanwhile, in case of the P type PT method where the transmitter and the receiver transducers are installed at the center of the top cap and the pedestal respectively, a constrained wave in longitudinal direction propagating in the rod is assumed. From this, the value of constrained modulus (M) is observed with Equation 5 and then for comparison the value of M is converted into the value of E using Equation 6, respectively as follows:

$$M = \rho \cdot V_P^2 \qquad (5)$$

$$E = \frac{M(1-2\nu)(1+\nu)}{(1-\nu)} \qquad (6)$$

where $\nu$ is Poisson's ratio (= 0.17 for Toyoura sand (Hoque, 1996)).

To compare the values among those moduli comprehensively, the values of E are converted to those of G considering the isotropic condition by employing Equation 7, as follows:

$$G = \frac{E}{2(1+\upsilon)} \qquad (7)$$

Additionally, to neglect the effects of density ($\rho$) or void ratio (e), the values of G are normalized with a void ratio function, f(e), that was proposed by Hardin and Richart (1963) as in Equation 8 as follows:

$$f(e) = \frac{(2.17-e)^2}{(1+e)} \qquad (8)$$

## TEST RESULTS AND DISCUSSIONS

### *Shear Modulus with Various Measurement Techniques*
All the graphs in Figures 3 to 7 are plotted between the normalized values of shear modulus (G/f(e)) versus the stress parameter. The hollow and solid symbols refer to the values of G/f(e) obtained with

the tests under dry and saturated conditions, respectively. Different values observed by different researchers are described with symbols in different shapes, instead of different colors.

Figure 3 shows the normalized values of statically measured shear modulus versus the stress parameter. The data were contributed by all the six researchers by employing triaxial and torsional apparatuses. All the data were plotted along the curve fitting with the deviation of about 3.7%.

Figure 4 shows the values of G/f(e) observed with bender element. In this study, S wave produced by the bender element propagated from top cap to pedestal through the soil. After performing simple linear regression, it was found that the values of $G_{BE}$ were spread with the deviation of 2.9%.

Figure 5 shows the values of G/f(e) resulted from TA with S wave. Using the tools of the TA with S, no significant difference of G/f(e) values was observed between those were combined with triaxial and those with torsional apparatus, except to those of data D1 showing distinctively higher values. However, all of the values excluding those of data D1 were fit to the linear curve with the deviation of 7.6%.

Figure 6 shows the values of G/f(e) observed by TA with P wave method. The values of data A2 seemed to be unreliable as compared to others to the fact that the values were observed with the specimen under saturated condition. It is occurred due possibly to that the velocity of P wave propagating inside the specimen under saturated condition is affected by the existence of pore water. By ignoring the values of data A2, those of $G_{TA-P}/f(e)$ were fit to the regression line with the deviation of 4.1%.
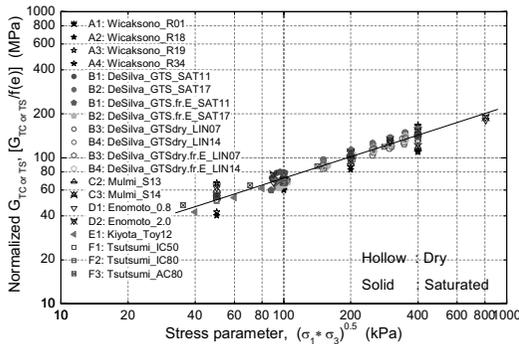


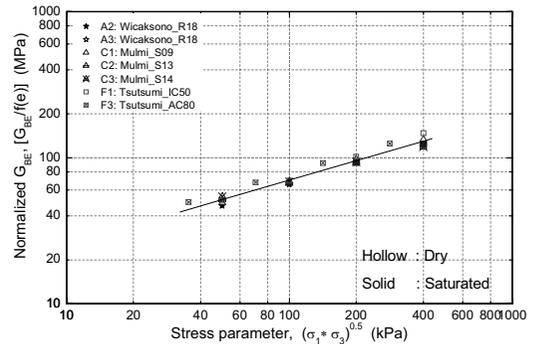Figure 3. Normalized $G_{TC \text{ or } TS}$ values versus stress parameter



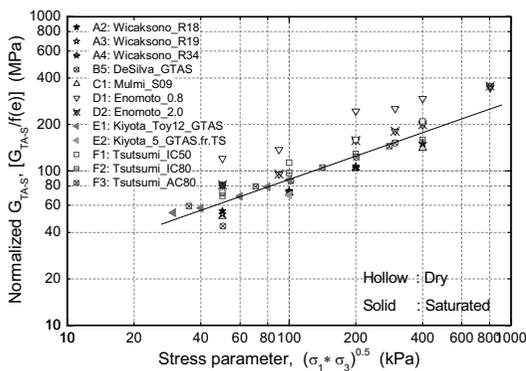Figure 4. Normalized $G_{BE}$ values versus stress parameter



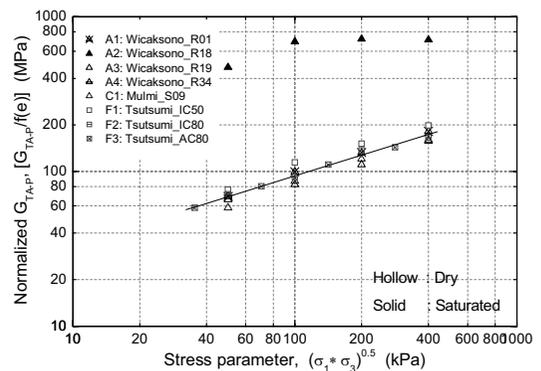Figure 5. Normalized $G_{TA-S}$ values versus stress parameter



Figure 6. Normalized $G_{TA-P}$ values versus stress parameter

Figure 7 shows the values of $G_{PT-S}/f(e)$ and $G_{PT-P}/f(e)$ versus the stress parameter. Since the tools of PT method are relatively new in this laboratory, to date only one researcher has been utilizing them to measured small strain stiffness. The values of $G_{PT-P}$ were obtained originally from those of $M_{PT-P}$ by considering Equation 6. However, the values of $G_{PT-S}/f(e)$ and $G_{PT-P}/f(e)$ seemed to be plotted in a good agreement having the deviation of 3.6%.

After comparing each data obtained from each method among the researchers, then the comprehensive comparison was performed to all the results showed in this study. For the simplicity, all of the data were represented by their fitting lines as shown in Figure 8. Three lines of shear modulus from the static, the BE, and the PT methods were in a good agreement. Meanwhile, the fitting lines of shear modulus from the TA method with S wave and that with P wave were in a good agreement. However, in average the values of shear modulus obtained with the TA methods resulted in about 30% higher than those with the BE and the PT methods.
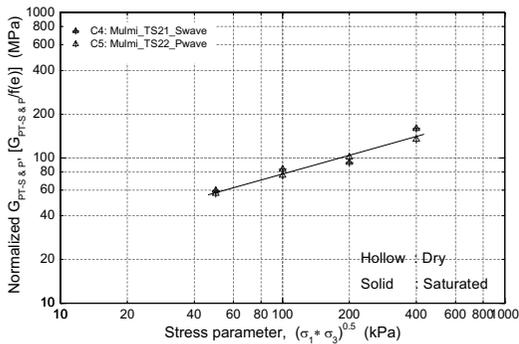


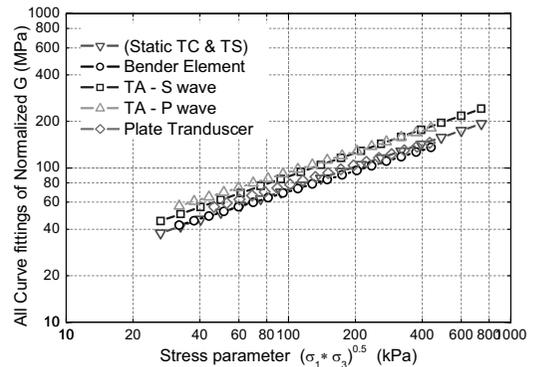Figure 7. Normalized $G_{PT-S \& P}$ values vs. stress parameter



Figure 8. All Curve Fittings of the data

The phenomenon of the values of shear modulus resulted from the TA measurements are larger than those resulted from the static measurement, is in accordance with the previous study on Toyoura sand and Hime gravel ($D_{50}$=1.7 mm) (Wicaksono, 2008). Maqbool (2005) inferred that the difference between statically and dynamically measured stiffness moduli is due possibly to the effects of heterogeneity of the specimen. Furthermore, AnhDan and Koseki (2002) found that the difference on dynamic and static properties is not only caused by strain level but also by some other factors like grain size and wave length.

Additionally, on coarser material (Hime gravel), the dynamic measurement using the BE method appears to underestimate as compared to that using the TA method is due possibly to the effects of bedding error at both the top-end and the bottom-end of the specimen. Nevertheless, it is not significant in case with Toyoura sand (Wicaksono, 2007b).

### Wave Propagation Measured Inside and Outside the Specimen
The facts obtained above may lead to the question on the reliability of TA methods which attaches accelerometers on the membrane on the side of specimen. Considering this, further study on TA methods was performed by putting the accelerometers both outside and inside the specimens.

Large scale triaxial apparatus was employed to conduct test R47 having the specimen size similar to that of test A4 (Table 1). As described by the schematic figures and photos shown in Figure 9, four accelerometers were installed inside the specimen having the position so that were possible to measure travel time of P and S waves, while usual manner of attaching accelerometers outside the specimen was also conducted for comparison. Cables of the inside accelerometers were managed to go out from the specimen through a hole at the pedestal like that of the drainage line. Similar to the common setting of TA method, two pairs of the accelerometers located inside and outside the specimens

respectively were set to capture the wave propagation simultaneously. Each pair of the accelerometers was put in 2 different locations (upper and lower) at certain vertical distance from the top cap.

As standard procedures in this study, after completing the cyclic loading stage, under constant stress stage the TA measurement was carried out. A series of elastic wave with several different frequencies generated by a function generator was employed. For comparison, in addition to those were produced by the function generator; a set of elastic wave was generated by hitting a hammer on the EDT pad attached to the loading piston (Figure 1).
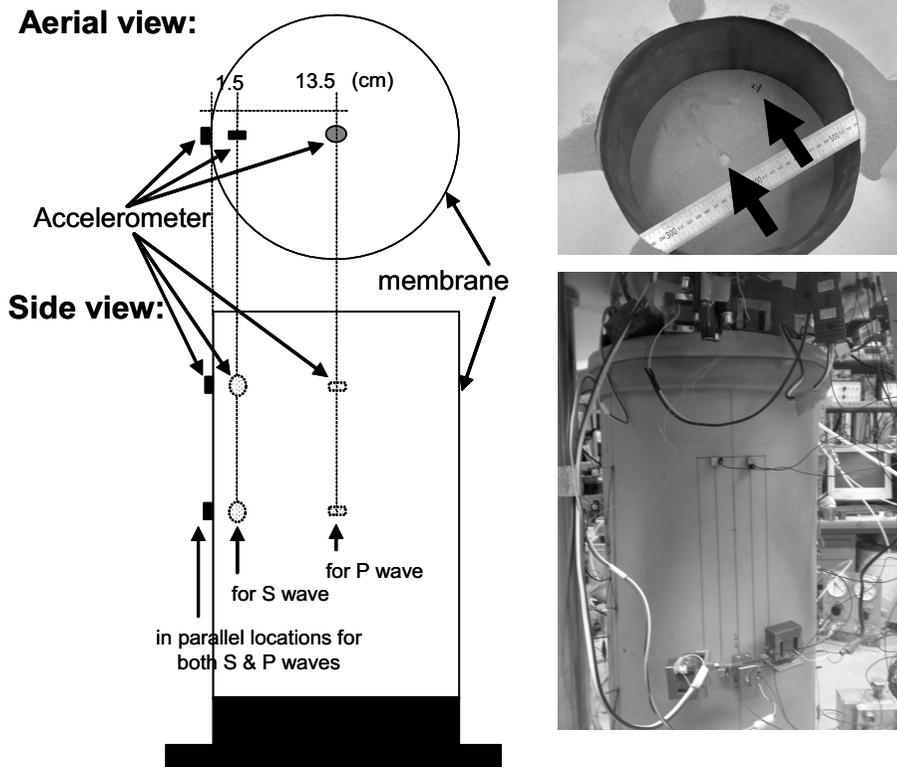


Figure 9. Schematic figures and photos for the location of the accelerometers

Figures 10 and 11 present the time history of wave propagation for both S and P waves with the wave sources of sine wave with 2 kHz in frequency and hitting by hammer, respectively. In those figures, the accelerometers defined with Ch.1 and Ch.2 are represented for those at upper and lower locations, respectively. Meanwhile, terms of "inside" and "outside" are used to indicate the accelerometers located inside and outside the specimens, respectively.

In general, faster wave velocity was observed in the waves measured inside the specimen as compared to those outside one. Despite Figure 10b shows that the rising point observed by the upper accelerometer located inside the specimen (Ch.1 - inside) was later than that located outside one (Ch.1 - outside), however by considering the first coming wave that assumed as near-field effects, the wave measured inside the specimen was still captured earlier. Meanwhile, with the P wave as shown in Figure 11, opposite polarities were observed between the first rising signal captured by the inside accelerometers and those by the outside ones. Those phenomena are not clear yet to be discussed until that more detailed and careful study observing the wave distribution on the cross section of the specimen is conducted.
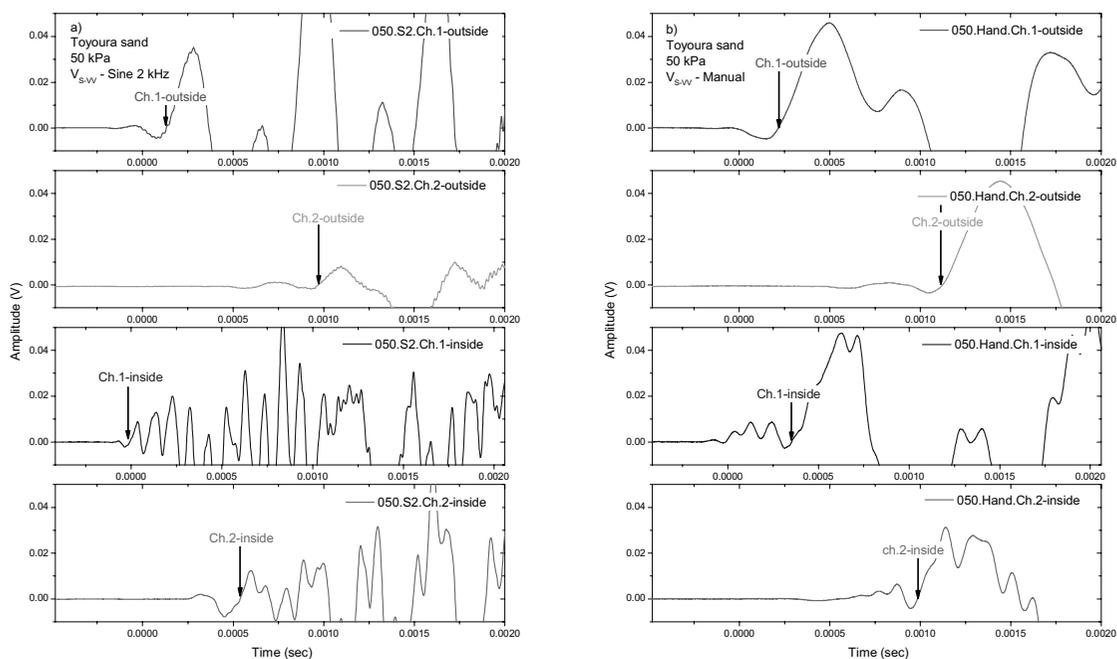
Figure 10. Time history of the input and the output $V_S$ waves: a) Sine 2 kHz; b) hit by hammer
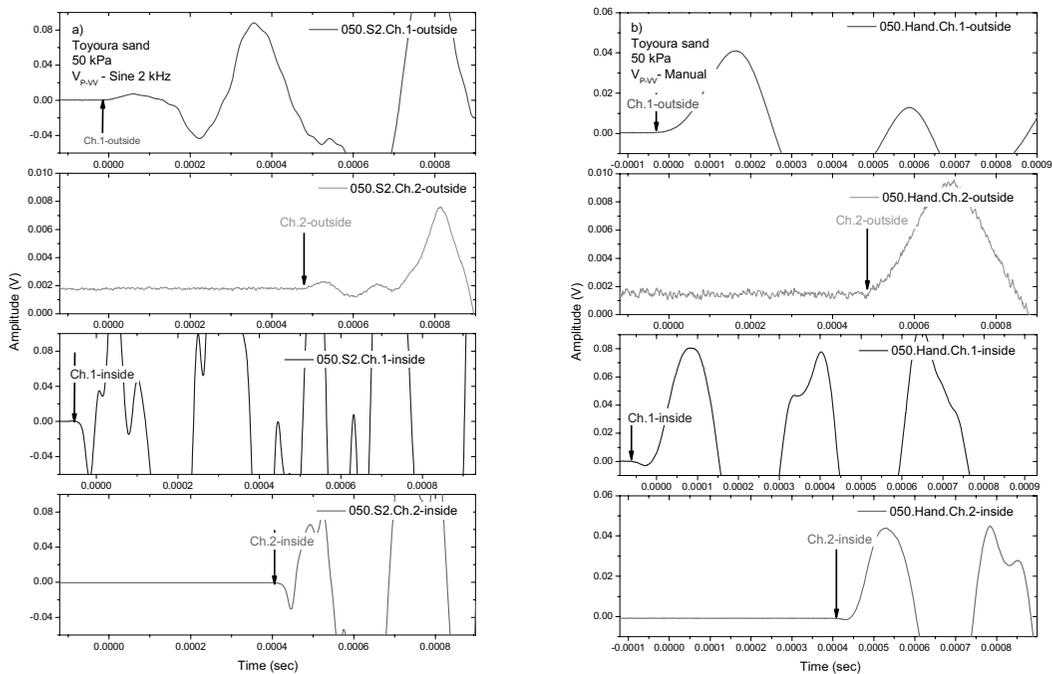


Figure 11. Time history of the input and the output $V_P$ waves: a) Sine 2 kHz; b) hit by hammer

As the results of wave velocity measured inside and outside the specimens, Figures 12a and 12b show graphs plotting the values of wave velocity versus the confining stress obtained from the TA method with S and P waves respectively. The graphs compare between those employing the accelerometers inside the specimen and those outside one. In general these results suggested that for both S and P waves, slightly faster velocity of the wave propagation measured inside the specimen was observed as compared to that outside one. The scattering values of S wave velocity ($V_S$) between those captured by the inside and the outside accelerometers were fit to the regression line with the deviation of 2.8%, while those of P wave velocity ($V_P$) were with the deviation of 2.6%.
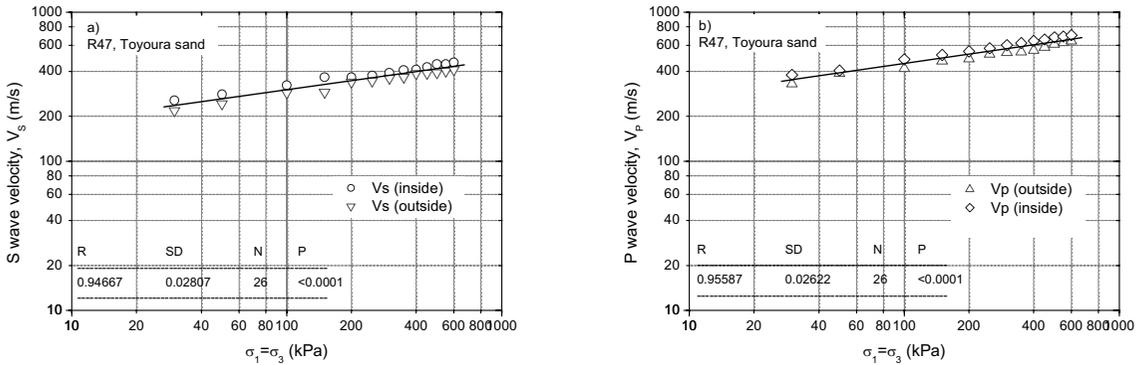


Figure 12. Wave velocity with accelerometers inside and outside the specimen: a) with TA-S wave; b) with TA-P wave

***Comparison with the Result from Round Robin Test***

In 2003, led by Japanese Geotechnical Society (JGS) the Technical Committee 29 (TC-29) of the Geomaterials of International Society of Soil Mechanics and Geotechnical Engineering (ISSMGE) that works on Stress-Strain and Strength Testing, started an international parallel test on the measurement of $G_{max}$ using bender element. By 2005, a report of this round robin test works collecting data from 23 institutions of 11 countries was published. In this study, the report resulted from the round robin test was used for further comparison.
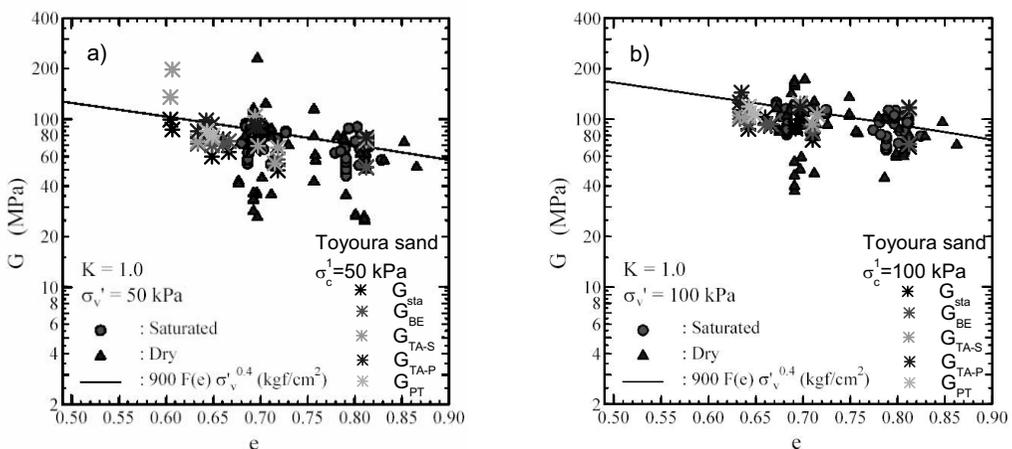


Figure 13. Comparison between results from this study and those from round robin test organized by TC-29, at the confining pressure ($\sigma'_c$) of: a) 50 kPa; b) 100 kPa
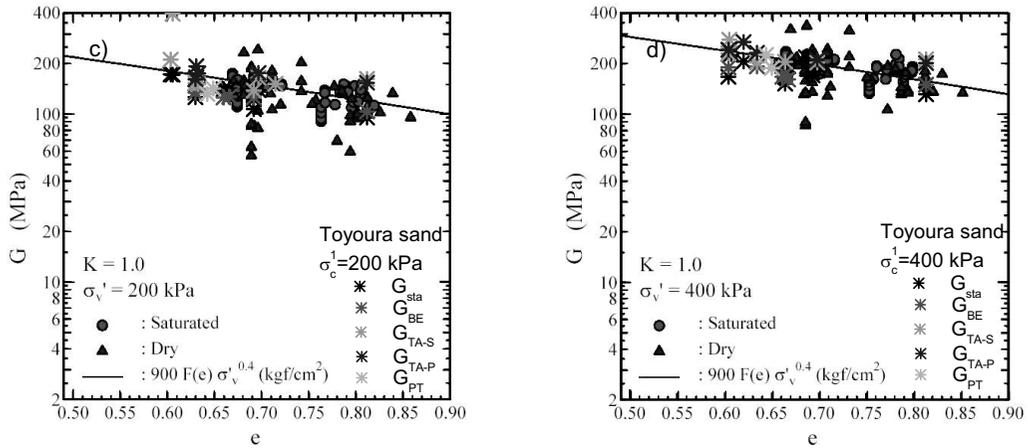
Figure 13 (continue). Comparison between results from this study and from round robin test organized by the TC-29, at the confining pressure ($\sigma'_c$) of: c) 200 kPa; d) 400 kPa

Figures 13a to 13d present the graphs of the comparison at the vertical stresses of 50, 100, 200, and 400 kPa, respectively. Data of this study are represented with star symbol with different colors for different measurement methods. It was observed that the results from this study were in a good agreement with those from the TC-29.

Considering the shear modulus values resulted from this study as presented in Figure 8, the fact was observed that those obtained from the TA methods were higher than those from other methods. However, when those of this study were compared with those of the TC-29 as shown in Figure 13, it seemed to that the scattering was plotted in the acceptable range. It suggests that by performing any techniques of small strain stiffness measurement especially on Toyoura sand, subjectively acceptable scattering on the shear modulus values is observed.

## CONCLUSIONS

By considering different researchers with various techniques (in terms of specimen sizes, densities, dry and saturated conditions, apparatuses), small strain measurements using static, Trigger Accelerometer (TA), Bender Element (BE) and Plate Transducer (PT) methods on Toyoura sand yielded the values of normalized shear modulus having the deviation at largest of about 7.6%. However, the values of shear modulus obtained with the TA methods resulted in about 30% higher than those with the BE and the PT methods.

Instantly, further study on the TA methods with both S and P waves confirmed that with the deviation of about 3% the velocity of the wave propagation measured inside the specimen was observed faster than that outside one. To explain complicated phenomena regarding wave propagation inside the specimen, further detailed and careful study is needed.

By plotting results from this study and those from International Parallel Test on the Measurement of $G_{max}$ using Bender Elements organized by the TC-29 in a graph for particular confining pressure, all of the G values seemed to be scattered in the acceptable range. The implication is that it suggests that by performing any methods of small strain stiffness measurement especially on Toyoura sand, subjectively acceptable scattering on the shear modulus values is observed.

**ACKNOWLEDMENT**

**REFERENCES**

AnhDan, L.Q., Koseki, J., and Sato, T. (2002) "Comparison of Young's Moduli of Dense Sand and Gravel Measured by Dynamic and Static Methods", *Geotechnical Testing Journal*, ASTM, Vol. 25 (4), pp. 349-368.

De Silva, L.I.N., Koseki, J., Sato, T., and Wang, L. (2005) "High capacity hollow cylinder apparatus with local strain measurements", *Proceedings of the Second Japan-U.S. Workshop on Testing, Modeling and Simulation, Geotechnical Special Publication*, ASCE, Vol. 156, pp. 16-28

Dyvik, R. and Madshus, C. (1985) "Laboratory Measurements of $G_{max}$ using Bender Elements", *Advance in the Art of Testing Soils under Cyclic Conditions*, ASCE, New York, 186-196.

Enomoto, T. (2008) "Small Strain Measurement on Toyoura Sand using Large Apparatus in IIS" (personal communication).

Goto, S., Tatsuoka, F., Shibuya, S., Kim, Y.S., and Sato, T., (1991) "A Simple Gauge for Local Small Strain Measurements in the Laboratory", *Soils and Foundations*, 31 (1), 169-180.

Hardin, B.O. and Richart, F.E.J. (1963) "Elastic Wave Velocities in Granular Soils", *Journal of Soil Mechanics and Foundation*,  ASCE, 89(1), pp. 33-65.

Hoque, E. (1996) *Elastic Deformation of Sands in Triaxial Tests*, Ph.D Thesis, University of Tokyo, Japan.

Japanese Domestic Committee for TC-29 (2005) *International Parallel Test on the Measurement of $G_{max}$ Using Bender Elements Organized by TC-29*, Japan.

Kiyota, T. (2008) "Small Strain Measurement on Toyoura Sand using Triaxial and Torsional Apparatus in IIS" (personal communication).

Lee, J.S. and Santamarina, J. (2005) "Bender Elements: Performance and Signal Interpretation", *Journal of Geotechnical and Geoenvironmental Engineering*, 131(9), 1063-1070.

Maqbool, S. (2005) *Effects of Compaction on Strength and Deformation Properties of Gravel in Triaxial and Plane Strain Compression Tests*, Ph.D Thesis, Dept. of Civil Engineering, The University of Tokyo, Japan.

Mohsin, A. and Airey, D. (2003) "Automating $G_{max}$ Measurement in Triaxial Tests", *Proceedings of 3rd International Symposium on Deformation Characteristics of Geomaterials*, Lyon, Di Benedetto H, Doanh T, Geoffroy H, Sauzeat C, eds., Vol. 1, Balkema, Lisse, 73-80.

Mulmi, S., Koseki, J., and Kuwano, R. (2008a) "Sample Size and Shape Effects in Bender Element Tests", *Proceedings of 10th IS Symposium*, JSCE, Japan, pp. 85-88.

Mulmi, S., Sato, T., and Kuwano, R. (2008b) "Performance of Plate Type Piezoceramic Tranducers for Elastic Wave Measurements in Laboratory Soil Specimens", *Seisan Kenkyu*, Vol. 60 No. 6, Japan, pp. 43-47.

Santamarina, J.C., in collaboration with Klein, K. and Fam, M. (2001) *Soils and Waves*, J. Wiley and Sons, Chichester, UK, 488 pages.

Stokoe, K.H. II. and Hoar, R.J. (1978) "Field Measurement of Shear Wave Velocity by Cross Hole and Down Hole Seismic Methods," *Proceedings of the Conference on Dynamic Methods in Soil and Rock Mechanics*, Karlsruhe, Germany, 3, 115-137.

Tanaka, Y., Kudo, K., Nishi, K., Okamoto, T., Kataoka, T., and Ueshima, T. (2000) "Small Strain Characteristics of Soils in Hualien, Taiwan," *Soils and Foundations*, Vol. 40 (3), pp. 111-125.

Tatsuoka, F. and Shibuya, S. (1991) "Deformation Characteristics of Soils and Rocks from Field and Laboratory Tests", Keynote Lecture for Session No.1, *Proceedings of the 9th Asian Regional Conference on SMFE*, Bangkok, Thailand, 2, pp.101-170.

Tatsuoka, F. and Shibuya, S. (1992) "Deformation Characteristics of Soils and Rocks from Field and

Laboratory Tests," *Proeedings. of 9th Asian Regional Conf. of SMFE*, Bangkok, Vol. 2, pp. 101-170.

Tatsuoka, F. and Kohata, Y. (1995) "Stiffness of Hard Soils and Soft Rocks in Engineering Applications", Keynote Lecture, *Proceedings of International Symposium Pre-Failure Deformation of Geomaterials* (Shibuya et al., eds.), Balkema, 2, pp. 947-1063.

Tsutsumi, Y., Builes, M., Sato, T., and Koseki, J. (2006) "Dynamic and Static Measurements of Small Strain Moduli of Toyoura Sand", *Bulletin of Earthquake Resistant Structure Research Center*, University of Tokyo, 39, pp.91-103.

Wicaksono, R.I. (2007a) *Small Strain Stiffness of Sand and Gravel Based on Dynamic and Static Measurements*, Master Thesis, Dept. of Civil Engineering, The University of Tokyo, Japan.

Wicaksono, R.I., Tsutsumi, Y., Sato, T., Koseki, J., and Kuwano, R. (2007b) "Small Strain Stiffness of Clean Sand and Gravel Based on Dynamic and Static Measurements", *Proceedings of 9th IS Symposium*, JSCE, Japan, pp. 171-174.

Wicaksono, R.I., Tsutsumi, Y., Sato, T., and Koseki, J,, Kuwano, R. (2008) "Laboratory Wave Measurement on Toyoura Sand and Hime Gravel", *Bulletin of Earthquake Resistant Structure Research Center*, University of Tokyo, Japan 41, pp.35-44.

Woods, R.D. (1991) "Field and Laboratory Determination of Soil Properties at Low and High Strains," *Proceedings of Second International Conference on Recent Advances in Geotechnical Earthquake Engineering and Soil Dynamics*, pp. 1727-1741